Adaptive classification on Brain Computer Interfaces using reinforcement signals

A. Llera Arenas[1, 2]

a.llera@donders.ru.nl

[1]Radboud University Nijmegen, the Netherlands

[2]Donders Institute for Brain, Cognition and Behaviour, Nijmegen, the Netherlands

V. Gómez[1, 2]

v.gomez@science.ru.nl

H. J. Kappen[1, 2]

b.kappen@science.ru.nl

Keywords: Adaptive classification, Brain computer interfaces.

Abstract

We introduce a probabilistic model that combines a classifier with an extra *Reinforcement Signal (RS)* encoding the probability of an erroneous feedback being delivered by the classifier. This representation computes the class probabilities given the task related features and the reinforcement signal. Using Expectation Maximization (EM) to estimate the parameter values under such a model shows that some existing adaptive classifiers are particular cases of such an EM algorithm. Further, we present a new algorithm for adaptive classification, we call it *Constrained means adaptive classifier (CMAC)*, and show using EEG data and simulated *RS* that this classifier is able to significantly outperform state-of-the-art adaptive classifiers.

1 Introduction

The final goal of a Brain Computer Interface (BCI) is to provide human subjects with control over some device or computer application only through their measured brain activity by e.g. electroencephalogram (EEG) (Wolpaw et al, 2002). To gain control over the device, the user usually participates in an off-line train/calibration session, where he/she is instructed to perform some mental task according to visual stimuli while the generated brain activity is being recorded (Ramoser et al, 1998; van Gerven et al, 2009). From the recorded data, discriminative features associated with the different intentions of the user are extracted and used to train a classifier which will predict the intention of the user during the test/feedback session.

However, due to the poor signal to noise ratio and the non stationary character of the EEG data (Krauledat, 2008), the patterns extracted during the training of the BCI may differ for the feedback session leading to a poor performance (Shenoy et al, 2006). It has been shown that to keep an acceptable performance, EEG based BCIs require a robustified feature space (Tomioka et al, 2006; Blankertz et al, 2008; von Bünau et al, 2010; Reuderink et al, 2011; Samek et al, 2012) and/or online adaptation of the classifier parameters (Millán, 2004; Shenoy et al, 2006). Since in practical BCI scenarios the user intention is unknown, online supervised adaptation is not possible, so the design of unsupervised adaptive classifiers that are robust to changes due to the non stationary character of the data has become focus of intense research within the BCI community (Sykacek et al, 2004; Gan, 2006; Kawanabe et al, 2006; Vidaurre et al, 2006; Hasan et al, 2009).

A common approach considers the class conditional features as normally distributed variables, and performs unsupervised adaptation of a Linear Discriminant Analysis (LDA) classifier. Adaptive LDA Pooled-mean (*Pmean*), and adaptive LDA Pooled-mean + Global Covariance (*PmeanGcov*) are two representative examples of this kind of methods (Vidaurre et al, 2010). Recently, interesting online experiments have shown the practical application of these techniques, not only for improving the performance with respect to static classifiers, but also for reducing the training time or increasing the amount of possible BCI users (Vidaurre et al, 2010b,c). Other methods model the user intention as a latent variable for which its posterior probabilities (responsibilities) are computed and subsequently used to update a classifier. This idea has been introduced using Expectation Maximization (EM) in Gaussian Mixture Models (GMM) in Blumberg et al (2007), and extended to sequential EM in Hasan et al (2009) and Liu et al (2010). Other extension for joint adaptive feature extraction and classification was considered in Li et al (2006).

A possible way to improve unsupervised adaptive methods consists of the use of a *re-*

inforcement signal (RS) which acts as a feedback provided by the user to the machine. Examples of *RS* can range from button presses delivered by the user (supervised), to measured muscular activity in an hybrid BCI (Leeb et al, 2010). Another relevant example of RS is the Error Related Potential (ErrP), a stereotyped pattern elicited following an unexpected response from the BCI (Ferrez, 2007; Ferrez et al, 2008). There is evidence that this signal can be detected with high accuracy (Chavarriaga et al, 2007, 2010; Blankertz et al, 2004; Llera et al, 2011). The inclusion of such a *RS* into the adaptive BCI cycle was introduced in Blumberg et al (2007). In that work, the authors extend the latent variable approach with an additional binary ErrP classifier. Similarly, in Llera et al (2011) we proposed a discriminant-based approach that also uses a binary ErrP classifier, and provided a detailed analysis of the negative effect due to false positives/negatives on the ErrP misclassification.

In this work we introduce a unifying framework which accommodates existing approaches in two families according to whether a latent variable is explicitly modeled or not. Our framework is derived from a graphical model which includes a probabilistic *RS* instead of a binary *RS*. This is a way to include the reliability over the measured *RS* which implements soft updates when the uncertainty is high, and recovers unsupervised and supervised learning as particular cases. Further, we develop a novel algorithm for adaptive classification and present an overview of the relations between existing methods.

In section 2.1 we introduce a probabilistic graphical model, describe the EM algorithm for estimating the parameters in this model, and derive its sequential version (*CSEM*).

In section 2.2 we develop a new sequential algorithm (*CMAC*) for classification and parameter estimation. In 3.1 we provide a description of the simulated *RS* which will be considered to evaluate the proposed methods. In sections 3.2 and 3.3 we present the results obtained using synthetic data. In section 4 we compare the proposed methods with other state of the art classifiers using EEG data and simulated *RS*. Then, in section 5 we give a brief description of the methods which are related to our work and describe the relationships and/or differences between the proposed and the previously existing methods. Finally, in section 6 we discuss the presented results and consider future work directions.

2 Methods

In section 2.1, we introduce a probabilistic graphical model which includes the task related features as well as a *Reinforcement Signal (RS)* encoding the discrepancy between the user intention and the output given by the device. This formulation estimates the posterior probabilities of each class (responsibilities) after observing not only the task related features but also the RS. We describe the *EM* algorithm for this model and derive a sequential version of it (*CSEM*). In 2.2 we derive a new algorithm for online parameter estimation and classification (*CMAC*), which can use the responsibilities computed including the *RS*.

2.1 The model

We consider a binary random variable $I \in \{1, 2\}$ representing the hidden intention of the user. Given the intention, a vector $\mathbf{x} \in \mathbb{R}^n$ represents the features extracted from the recorded brain activity of the user while having intention I. Based on these features, a probabilistic *task classifier* is used to compute the output of the BCI, $Z \in \{1, 2\}$, which is used for control. The output Z can be interpreted as a feedback from the BCI to the user. Further, once Z is observed by the user, we consider a probabilistic *RS* which provides the probability of an erroneous feedback, $E \in [0, 1]$. Given Z and E as evidence, we can use the fact that I is a binary variable and write its conditional probability as:

$$p(I|Z,E) = \begin{cases} 1 - E & \text{if } I = Z \\ \\ E & \text{if } I \neq Z \end{cases} . \tag{1}$$

For simplicity, we will not explicitly consider the dependence of Z on $\mathbf{x}$ through the task classifier, nor the dependence of E on Z through the brain activity measured after observing Z and the *RS*. Instead, although the intention of the user is not actually caused by Z and E, we summarize the influence of Z through E as given by (1). Figure 1 shows a Bayesian network that captures the probabilities described above.

The joint probability distribution of the proposed model is

$$p(I, \mathbf{x}, Z, E) = p(\mathbf{x}|I)p(I|Z,E)p(Z)p(E). \tag{2}$$

We consider $p(I|Z,E)$ as given by (1), and assume normally distributed features given the intention, that is

$$p(\mathbf{x}|I) = \frac{1}{(2\pi)^{n/2}|\Sigma_I|^{1/2}} \exp\left(-\frac{1}{2}\left(\mathbf{x} - \boldsymbol{\mu}_I\right)^\intercal \Sigma_I^{-1}\left(\mathbf{x} - \boldsymbol{\mu}_I\right)\right) \equiv \mathcal{N}(\mathbf{x}|\boldsymbol{\mu}_I, \boldsymbol{\Sigma}_I),$$

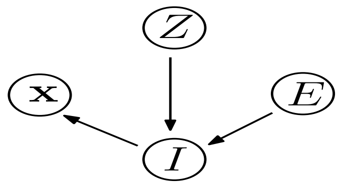

.

Figure 1: Probabilistic graphical model: $\mathbf{x} \in \mathbb{R}^n$ represents the task related features extracted from the EEG data, $Z \in \{1, 2\}$ the BCI output computed using the task classifier, $E \in [0, 1]$ the *RS* encoding the probability that Z was an erroneous output and $I \in \{1, 2\}$ denotes the intention of the user.

with the intention I replaced with a mean vector $\boldsymbol{\mu}_I \in \mathbb{R}^n$ and covariance matrix $\boldsymbol{\Sigma}_I \in \mathbb{M}_{n\times n}$ as sufficient statistics. Further, we will assume a flat prior over E and Z, so $p(E) = 1, \forall E \in [0, 1]$, and $p(Z) = \frac{1}{2}, \forall Z \in \{1, 2\}$. We compactly represent the set of parameters of the model using the vector $\boldsymbol{\theta} := (\boldsymbol{\mu}_1, \boldsymbol{\Sigma}_1, \boldsymbol{\mu}_2, \boldsymbol{\Sigma}_2)$.

Suppose that we have a data set of observations $\mathcal{S}$ from which we can estimate the unknown model parameters $\boldsymbol{\theta}$. In our case, the observations correspond to T trials that are composed of an observed component $\mathcal{S} = \{\langle \mathbf{x}^t, Z^t, E^t \rangle\}_{t\in\{1,\ldots,T\}}$, and a latent variable I^t, the intention at trial t. The log-likelihood of the data given the model parameters can be written as

$$\log p(\mathcal{S}|\boldsymbol{\theta}) = \sum_{t=1}^{T} \log \sum_{I^t=1}^{2} p(I^t, \mathbf{x}^t, Z^t, E^t|\boldsymbol{\theta}) = \sum_{t=1}^{T} \log \sum_{I^t=1}^{2} p(\mathbf{x}^t|I^t)p(I^t|Z^t, E^t)p(Z^t)p(E^t). \tag{3}$$

Maximizing (3) is not straightforward, since the summation over the latent variables I^t occurs inside of the logarithm. Typically, the Expectation Maximization (EM) algorithm is used to solve this problem (Bishop, 2007). The EM algorithm is a procedure which iterates two steps until convergence.

In the E-Step, one assumes current parameter values $\boldsymbol{\theta}^{\text{old}}$ and computes the posterior distribution of each of the intentions $I^t \in \{1, 2\}$, the so-called responsibilities:

$$p(I^t|\mathbf{x}^t, Z^t, E^t, \boldsymbol{\theta}^{\text{old}}) = \frac{p(\mathbf{x}^t|I^t, \boldsymbol{\theta}^{\text{old}})p(I^t|Z^t, E^t)}{\sum_{I^t=1}^{2} p(\mathbf{x}^t|I^t, \boldsymbol{\theta}^{\text{old}})p(I^t|Z^t, E^t)} \equiv \gamma_I^t. \tag{4}$$

In the M-step, we replace the old parameter values with the ones that result of maximizing the expected log-likelihood:

$$\boldsymbol{\theta}^{\text{new}} = \arg\max_{\boldsymbol{\theta}} \sum_{t=1}^{T} \sum_{I^t=1}^{2} p(I^t|\mathbf{x}^t, Z^t, E^t, \boldsymbol{\theta}^{\text{old}}) \log p(I^t, \mathbf{x}^t, Z^t, E^t|\boldsymbol{\theta}). \tag{5}$$

Taking derivatives of (5) with respect to the elements of $\boldsymbol{\theta}$ and setting them to zero results in the updates

$$\boldsymbol{\mu}_I = \frac{1}{N_I} \sum_{t=1}^{T} \gamma_I^t \mathbf{x}^t, \tag{6}$$

$$\boldsymbol{\Sigma}_I = \frac{1}{N_I} \sum_{t=1}^{T} \gamma_I^t (\mathbf{x}^t - \boldsymbol{\mu}_I)(\mathbf{x}^t - \boldsymbol{\mu}_I)^\intercal. \tag{7}$$

where $N_I = \sum_{t=1}^{T} \gamma_I^t$.

Note that this representation (Figure 1) computes the posterior probability of each of the intentions given the task related features and the *RS*. As a consequence, the difference between the proposed methodology and the standard EM for GMM relies on the use of $p(I^t|\mathbf{x}^t, Z^t, E^t, \boldsymbol{\theta}^{\text{old}})$ (4), a *RS* dependent quantity, instead of simply

$$p(I^t|\mathbf{x}^t, \boldsymbol{\theta}^{\text{old}}) = \frac{p(\mathbf{x}^t|I^t, \boldsymbol{\theta}^{\text{old}})}{\sum_{I^t=1}^{2} p(\mathbf{x}^t|I^t, \boldsymbol{\theta}^{\text{old}})}. \tag{8}$$

It is interesting to see that the model recovers the two following well-known cases:

Unsupervised case : If the *RS* is non-informative, $E^t = 1/2$, the updates become the ones of the EM for GMM.

Supervised case : If the *RS* is always correct and returns only a binary answer $E^t \in \{0, 1\}$, the responsibility of the incorrect intention is zero, whereas the responsibility of the correct intention is one.

Using the responsibilities as defined in (4), we can *interpolate* between unsupervised and supervised learning using the *RS*. This suggests an improvement over the unsupervised method given that the *RS* is informative. We show evidence for this later in section 3.2.

In the case that we have an incoming stream of data, as it is the case for online BCI, the previous optimization might not be efficient since it uses a batch of data and an iterative procedure in order to optimize the model parameters. For online BCI an incremental approach is necessary (Hasan et al, 2009b). A sequential version of the previously described EM algorithm is defined by the updates

$$\boldsymbol{\mu}'_I = (1 - \beta_\mu \gamma_I)\boldsymbol{\mu}_I + \beta_\mu \gamma_I \mathbf{x}, \tag{9}$$

$$\boldsymbol{\Sigma}'_I = (1 - \beta_\Sigma \gamma_I)\boldsymbol{\Sigma}_I + \beta_\Sigma \gamma_I (\mathbf{x} - \boldsymbol{\mu}_I)(\mathbf{x} - \boldsymbol{\mu}_I)', \tag{10}$$

where $\mathbf{x}$ is the observed task related feature vector, γ_I are the responsibilities computed using (4) and, β_μ and β_Σ *learning rates*. We will denote this algorithm as corrected sequential EM (CSEM).

2.2 Constrained Means Adaptive Classifier (*CMAC*).

In this section we develop the *Constrained Means Adaptive Classifier (CMAC)* algorithm for online classification and parameter estimation, a novel sequential update for the model parameters $\boldsymbol{\theta}$ which will allow for different rates of adaptation for shifts and rotations.

When no labels are available (unsupervised case) one can update a global mean of the data $(\mu_1 + \mu_2)/2$ by means of the learning rule

$$\frac{\boldsymbol{\mu}'_1 + \boldsymbol{\mu}'_2}{2} = (1-\beta)\frac{\boldsymbol{\mu}_1 + \boldsymbol{\mu}_2}{2} + \beta\mathbf{x}, \tag{11}$$

where $\boldsymbol{\mu}'_I$ represents the updated $\boldsymbol{\mu}_I$, $\beta \in [0,1]$ is the learning rate controlling the adaptation and $\mathbf{x}$ is the observed task related feature vector. This update rule can be seen as a constraint over the sum of the means and it was introduced in (Vidaurre et al, 2010). In terms of a discriminant function, this learning rule updates of the bias term. Despite its simplicity, this learning rule has been shown to be able to reliably keep track of the bias, significantly improving the classification accuracy wrt an static classifier. We generalize this rule and obtain an update for each of the means independently, which in terms of a LDA discriminant function will allow to update both the bias and the weights of the discriminant function. Consider an update rule for the means of the form

$$\boldsymbol{\mu}'_I = (1-\beta)\boldsymbol{\mu}_I + 2\beta\gamma_I\mathbf{x}, \tag{12}$$

where $\boldsymbol{\mu}'_I$ represents the updated $\boldsymbol{\mu}_I$, $\beta \in [0,1]$ is the learning rate controlling the adaptation, $\mathbf{x}$ is the observed task related feature vector and γ_I are the responsibilities computed using equation (4). A well known fact from online learning in changing environments (Heskes et al, 1991, 1992), is that the optimal learning rate depends on the noise as well as on the rate of change on the data. Under the assumption (12), the difference of the means depends on the responsibilities, while the sum does not. Therefore, the sum can be adapted more reliably than the difference, i.e. using larger learning rates. Extending equation (12) for the case of different learning rates ($\beta_+ > \beta_-$) for the sum and the difference of the means respectively, results in

$$\boldsymbol{\mu}_1' + \boldsymbol{\mu}_2' = (1 - \beta_+)(\boldsymbol{\mu}_1 + \boldsymbol{\mu}_2) + 2\beta_+ \mathbf{x}, \tag{13}$$

$$\boldsymbol{\mu}_2' - \boldsymbol{\mu}_1' = (1 - \beta_-)(\boldsymbol{\mu}_2 - \boldsymbol{\mu}_1) + 2\beta_-(\gamma_2 - \gamma_1)\mathbf{x}. \tag{14}$$

Solving for $\boldsymbol{\mu}_1'$ and $\boldsymbol{\mu}_2'$ gives the final updates for the means, which are shown in equations (15) and (16) in algorithm 1. To update the covariances, we use the updated means and the learning rule (10), where the learning rate $\beta_\Sigma \in [0, 1]$ controls the adaptation of the covariances. The full CMAC algorithm is described in algorithm 1. The initial parameters required by this algorithm can be obtained from a previous train/calibration session.

3 Results: Synthetic data

In this section we first explain the way in which the *RS* will be simulated in the rest of this work. In the rest of the section we show that using the responsibilities obtained by including the *RS* can improve the quality of the parameter estimation wrt an unsupervised GMM estimation, and then we perform a simulated online scenario to identify the kind of non stationarities *CMAC* is able to deal with while considering different *RS*'s.

3.1 The simulated *Reinforcement Signal (RS)*

By definition, the *RS* encodes the probability of presence of an error, so $E \in [0, 1]$. Thus, an informative *RS* should provide at each trial a value E, such that $E \approx 0$ for

Algorithm 1 *Constrained Means Adaptive Classifier (CMAC)*

```
Require: Current model parameters $\{\boldsymbol{\mu}_I , \boldsymbol{\Sigma}_I\}_{I\in\{1,2\}}$.
    Currently observed feature vector at present trial $t$, $\mathbf{x}^t$.
    Reinforcement Signal $E^t$ (after observing the output of the task classifier $Z^t$).
    Parameters controlling the adaptation $\beta_+$, $\beta_-$, $\beta_\Sigma$.
1: $\Sigma := \frac{\Sigma_1+\Sigma_2}{2}$.
2: Compute the output of the task classifier at trial $t$ as:
       $Z^t = \arg\max_I p(I|\mathbf{x}^t, \boldsymbol{\mu}_I, \boldsymbol{\Sigma}) := \arg\max_I p(\mathbf{x}^t|\boldsymbol{\mu}_I, \boldsymbol{\Sigma})$.
3: Observe $E^t$ and evaluate the responsibilities using (4) and (1) :
       $\gamma^t_{Z^t} = \frac{\mathcal{N}(\mathbf{x}^t|\boldsymbol{\mu}_{Z^t}, \boldsymbol{\Sigma})(1-E^t)}{\mathcal{N}(\mathbf{x}^t|\boldsymbol{\mu}_{Z^t}, \boldsymbol{\Sigma})(1-E^t) + \mathcal{N}(\mathbf{x}^t|\boldsymbol{\mu}_{\neg Z^t}, \boldsymbol{\Sigma})E^t}$.
       $\gamma^t_{\neg Z^t} = 1 - \gamma^t_{Z^t}$.
4: Update the model parameters:
       $\boldsymbol{\mu}'_1 = (1 - \frac{\beta_+ + \beta_-}{2})\boldsymbol{\mu}_1 + \frac{\beta_- - \beta_+}{2}\boldsymbol{\mu}_2 + \left(\beta_+ - \beta_-(\gamma^t_2 - \gamma^t_1)\right)\mathbf{x}^t$.   (15)
       $\boldsymbol{\mu}'_2 = (1 - \frac{\beta_+ + \beta_-}{2})\boldsymbol{\mu}_2 + \frac{\beta_- - \beta_+}{2}\boldsymbol{\mu}_1 + \left(\beta_+ + \beta_-(\gamma^t_2 - \gamma^t_1)\right)\mathbf{x}^t$.   (16)
       $\boldsymbol{\Sigma}'_I = \left(1 - \beta_\Sigma\gamma^t_I\right)\boldsymbol{\Sigma}_I + \beta_\Sigma\gamma^t_I(\mathbf{x}^t - \boldsymbol{\mu}_I)(\mathbf{x}^t - \boldsymbol{\mu}_I)^\intercal, \forall I \in \{1,2\}$.   (17)
5: return Updated parameters: $\{\boldsymbol{\mu}'_I, \boldsymbol{\Sigma}'_I\}_{I\in\{1,2\}}$.
```

correctly classified trials and $E \approx 1$ for erroneously classified trials. Obviously no *RS* is totally reliable, and violations of this conditions are due to false positives/negatives of the *RS*. In order to illustrate such an scenario, we model $p(E)$ as a symmetric mixture of beta distributions:

$$p(E) = \frac{1}{2}\left(\beta(E|w_1, w_2) + \beta(E|w_2, w_1)\right), \tag{18}$$

where

$$\beta(E|w_1, w_2) = \frac{E^{w_1-1}(1-E)^{w_2-1}}{\int_0^1 z^{w_1-1}(1-z)^{w_2-1}dz}$$

for some $(w_1, w_2) \in \mathbb{R}^+ \times \mathbb{R}^+$.

Making use of the output delivered by the task classifier Z and the real intention of the user I, we define $p(E|I = Z) := \beta(E|w_1, w_2)$ and $p(E|I \neq Z) := \beta(E|w_2, w_1)$ with $w_1 < w_2$. In this way, at each trial, E is generated by drawing a sample from $p(E|I = Z)$ if the trial was correctly classified, and from $p(E|I \neq Z)$ otherwise.

As an illustration, in the second row of figure 2, we show three different examples of the resulting density functions for $(w_1, w_2) \in \{(1, 5), (2.5, 5), (4, 5)\}$ respectively. This parameterization results in a Bayes classification error of the RS of approximately 5%, 20% and 40% respectively.

Summarizing, the presented parametrization allows for the simulation of a probabilistic *RS* whose accuracy can be controlled by means of the values of (w_1, w_2). Note that the supervised case is an extreme scenario in which the beta distributions became delta peaks at zero or one.

3.2 Batch learning

We start by generating a data set $\mathcal{S} = \{\langle \mathbf{x}^t, Z^t, E^t \rangle\}_{t \in \{1,\dots,T\}}$. We consider for simplicity a two dimensional feature space and generate consequently the task related features $\{\mathbf{x}^t\}_{t\in\{1,\dots,T\}}$ by sampling with the same probability from two Gaussian distributions with parameters $\bar{\boldsymbol{\mu}}_I \in \mathbb{R}^2$ and $\bar{\boldsymbol{\Sigma}}_I \in \mathbb{M}_{2\times 2}$, $I \in \{1,2\}$. Each sample $\mathbf{x}^t$ is classified as $Z^t = \arg\max_I p(I|\mathbf{x}^t, \tilde{\boldsymbol{\mu}}_I, \tilde{\boldsymbol{\Sigma}}_I)$, where the values for $\tilde{\boldsymbol{\mu}}_I$ are chosen randomly and $\tilde{\boldsymbol{\Sigma}}_I = \mathbb{I}_{2\times 2}$. Then we generate the *RS* outputs by drawing for each trial one sample E^t from $p(E|I = Z)$ if the trial was correctly classified and from $p(E|I \neq Z)$ otherwise as explained in 3.1. Once the data set $\mathcal{S}$ is defined, we iterate equations (4), (6) and (7) until convergence of the log-likelihood (5).

To evaluate the quality of the solutions obtained, we can compare their log-likelihood with the one obtained applying an unsupervised EM algorithm for GMM (analytically equivalent to $E^t = \frac{1}{2}\ \forall t$ in our model), and with the supervised case (analytically equivalent to the proposed model using a *RS* which at each trial produces an output $E^t = 1 - \delta_{I^t, Z^t}$, with I^t the real intention at trial t).

In the first row of Figure 2 we plot the log-likelihood of the parameters obtained at each iteration of the algorithm for the supervised case (dotted line), unsupervised case (continuous line) and the proposed model including the simulated *RS* (discontinuous line). In this case, to account for variations in learning due to different realizations of the *RS*, the presented results are the average over 100 realizations of the experiment, and the shadowed area describes the standard deviation around the plotted mean solution. The three plots reflect the different behavior of the model while considering three different *RS* corresponding with the three parameterizations of $p(E|I, Z)$ plotted in the second

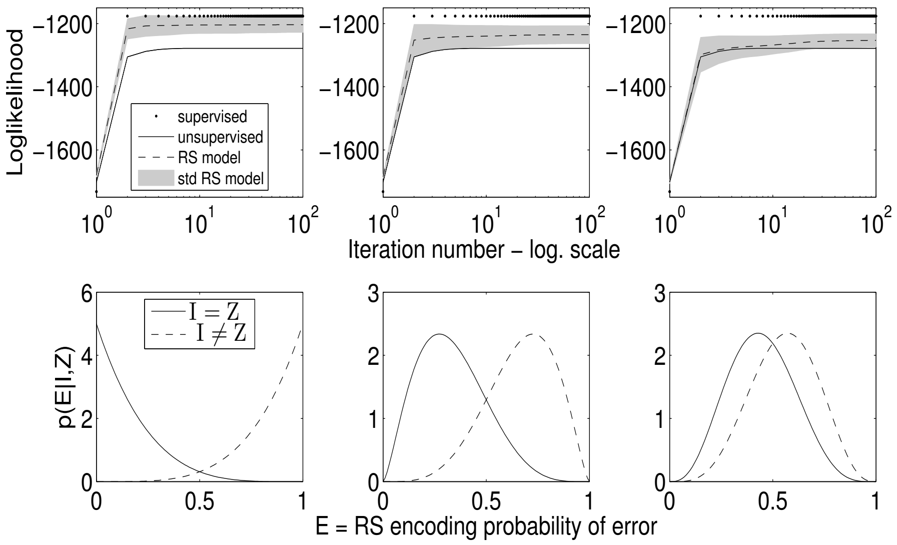

Figure 2: First row: Log-likelihood of the solutions obtained at each iteration for the unsupervised case (continuous line), supervised case (dotted line), and the proposed model (discontinuous line). The three horizontal plots show the different results obtained considering three different levels of accuracy of the *RS* corresponding with the parameterizations of $p(E|I,Z)$ shown in the second row.

Second row: $p(E|I,Z)$ is represented for 3 different parametrization of mixtures of β distributions. Continuous lines show $p(E|I = Z)$, discontinuous lines $p(E|I \neq Z)$. From left to right, the parameters for $(w1, w2)$ were set to $\{(1,5),(2.5,5),(4,5)\}$ respectively.

row.

For this illustration we considered $T = 100$,

$$\bar{\boldsymbol{\mu}}_1 = (1,1), \bar{\boldsymbol{\mu}}_2 = (2,-1), \bar{\boldsymbol{\Sigma}}_1 = \begin{pmatrix} 2 & 1 \\ 1 & 2 \end{pmatrix}, \bar{\boldsymbol{\Sigma}}_2 = \begin{pmatrix} 3 & 2 \\ 2 & 3 \end{pmatrix},$$

and the parameters were initialized as $\boldsymbol{\mu_1} = \tilde{\boldsymbol{\mu_1}}$, $\boldsymbol{\mu_2} = \tilde{\boldsymbol{\mu_2}}$ and $\boldsymbol{\Sigma_I} = \mathbb{I}_{2\times 2}$. However, the results obtained are not critically dependent on the choice of the parameters.

Note that the log-likelihood in the supervised scenario is the highest, and the solutions obtained using the proposed *RS* model improve the ones obtained in the unsupervised case for all considered *RS*. Further, as the *RS* becomes more reliable, the log-likelihood of the solutions is higher. This occurs because the *RS* is able to correct the responsibilities for the wrongly classified trials, either because they lie close to the decision boundary, or because they would have been wrongly assigned a large responsibility in the standard unsupervised sense.

These results confirm that this model allows to interpolate between the unsupervised and the supervised parameter estimation with the help of the *RS*, and additionally that the responsibilities computed using (4) provide a more accurate class measure than the responsibilities computed using (8).

3.3 CMAC - online learning behavior

We consider now two simulated online scenarios in which the underlying feature distributions are modified from the train session to the test session by means of a rotation and a translation of the optimal decision boundaries. These simulations provide insight on which kind of non stationarities can be captured by the proposed algorithm *CMAC*. In figure 3, black and grey curves represent the distributions of two different classes. Each row represents a different situation; the left most column shows the situation at the beginning of the test session, with the continuous curves representing the distributions of the test features while the discontinuous curves represent the distributions of the train features. In the first row there is a rotation between train and test distributions, while the second row there is a shift of the distributions.

Columns 2 to 5 show the test distributions (continuous lines) and the learned distributions using CMAC (discontinuous curves) under the assumption of different *RS* after generating 100 samples by sampling with the same probability from both test distributions. For the cases of 60 % and 80 % of accuracy of the *RS*, the results are the average over 100 realizations of the experiment. The standard deviation of these results was considered not significant for visualization. In this example, the parameter values were fixed to the values $\beta_+ = 0.05$, $\beta_- = 0.005$ and $\beta_\Sigma = 0.01$; The choice of this parameters do not change drastically the results in terms of the obtained solution.

Note that in the case of a translation of the distributions (second row), the new distributions can be estimated without the use of any *RS*. On the other hand, if a rotation of the distributions occurred (first row), a *RS* is necessary, and the estimation improves with the quality of the *RS*. This result is due to the fact that in order to correct for a rotation in the optimal decision boundary, the weights of the discriminant function need to be updated, and that requires the class label information.

4 Results: EEG data

In this section we use EEG data to perform a comparison between *CMAC* and other classifiers.

The EEG data was recorded from 6 subjects who participated in an experiment performing a binary motor imagery task (left-right hand) according to visual stimuli. Each subject participated in a calibration measurement consisting of 35 trials per class where no feedback was delivered, and two test sessions of 70 trials each where the feedback

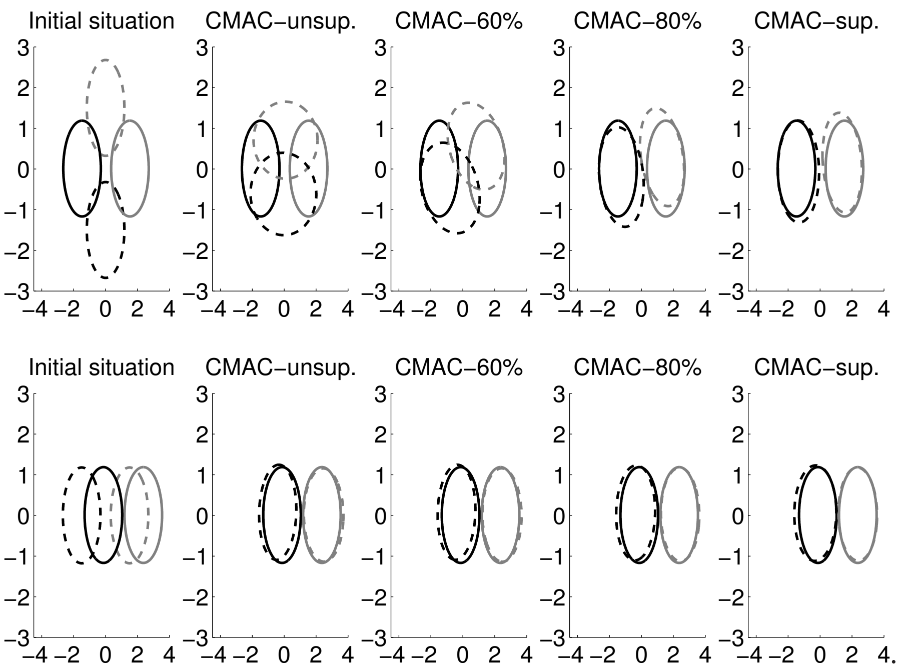

Figure 3: Black and grey curves represent the distributions of two different classes. Each row represents a different change in the feature distributions, a rotation in the first row and a shift in the second. The left column represents the situation at the beginning of the test session, with discontinuous lines representing the train features distributions and continuous lines the test features distributions. Columns 2 to 5 show the test features distributions (continuous lines) and the learned distributions using CMAC (discontinuous lines) under the assumption of different *RS* after 50 samples were drawn from each of the test feature distributions.

was delivered to the user in the form of a binary response. See Figure 4 for more detailed information about the experiment design. Between each two sessions there was a pause of 5 minutes.

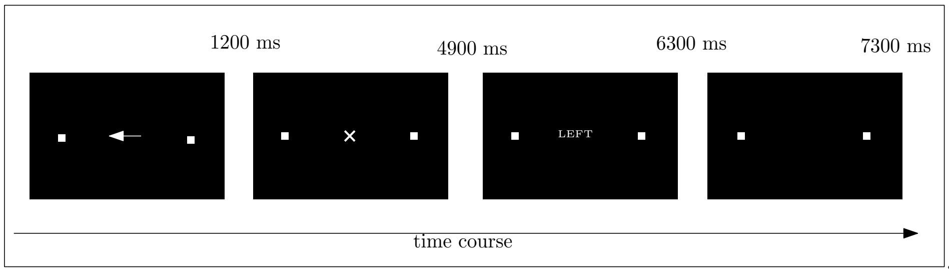

Figure 4: Experimental protocol during each trial of the test sessions: From time $0-1200$ ms an arrow indicates the side to which the task must be performed. After this period, a fixation cross is presented ($1200-4900$ ms) indicating the period to perform the task. At the end of this period, the device returns feedback to the user ($4900-6300$ ms), and it is followed by 1000 ms of no activity previous to the beginning of a new trial. During the calibration measurement the protocol was identical with the exception that no feedback was returned.

The brain activity was recorded using a multi-channel EEG with 64 electrodes at 2048 Hz. The data was down sampled at 250 Hz and made into trials using at each trial the data from the imaginary movement period ($1200-4900$ ms). An automatic variance based routine was applied to remove noisy trials and channels. The data was then linearly detrended and bandpass filtered in the frequency band $8-30$ Hz since these have been previously reported as the frequencies of main interest (Müller-Gerking et al, 1998). Common Spatial Patterns (CSP) (Fukunaga, K. , 1990; Lemm et al, 2005) were computed using the data from the calibration session, and the number of selected filters was three from each side of the spectrum. After projecting each trial to the space generated by the six filters, the logarithm of the normalized variance of these projections were used as features, resulting in a feature space of dimension 6.

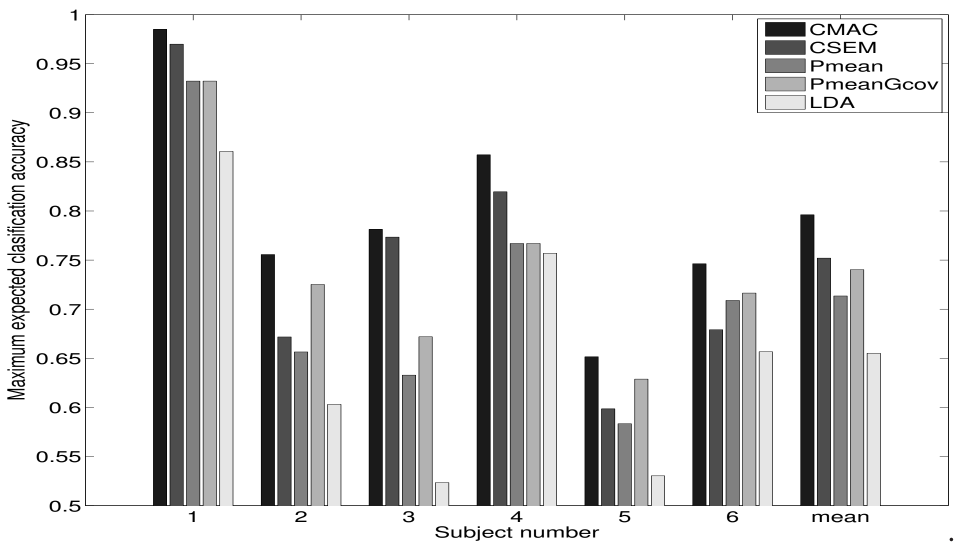

Figure 5: Maximum performance achievable using CMAC, CSEM, Pmean, PmeanGcov, as well as the performance obtained using LDA.

In the remaining of this section we use the previously described data set to perform a comparison between different classifiers, including a static classifier, *LDA* (Fukunaga, K. , 1990), and the adaptive classifiers *Pmean*, *PmeanGcov*, *CSEM* and *CMAC*. We first study the best possible performance obtained while using each of the considered methods. Figure 5 shows the maximum classification accuracy (number of correctly classified trials divided by the total number of trials) obtained by each method while considering optimized learning rates and an optimal *RS*. For each algorithm and each subject, the learning rates were optimized using grid search in parameter space.

First note that all adaptive classifiers are able to outperform *LDA*. From the adaptive classifiers, *CMAC* is clearly the algorithm able to reach the highest accuracy, followed by *CSEM* and *PmeanGcov* which reflect a similar performance. In the case of *Pmean*,

	CMAC $\beta_+, \beta_-, \beta_\Sigma$	CSEM β_μ, β_Σ	PmeanGcov β_μ, β_Σ	Pmean β_μ
Mean	$0.068, 0.019, 0.035$	$0.019, 0.069$	$0.019, 0.063$	0.084
Standard Deviation	$0.079, 0.011, 0.062$	$0.014, 0.049$	$0.014, 0.041$	0.073

Table 1: Mean across subjects and standard deviation of the optimal learning rates for each of the considered adaptive classifiers

we see that the model with less parameters (only one learning rate), is the one achieving the lowest accuracy but it is still able to clearly outperform *LDA*. This result clearly shows that *CMAC* has the potential power to outperform all other considered methods. As a reference for the reader, in table 1 we show the mean (across subjects) and standard deviation of the optimal parameter values set for each of the considered adaptive classifiers.

In practice, we do not have prior access to the optimal learning rates and furthermore, no *RS* is optimal. Clearly, different choices for the learning rates will affect the performance of all methods and moreover, suboptimal *RS* will affect the performance of *CMAC* and *CSEM*. In Figure 6 we present the performance of each of the methods as a function of different *RS* simulated as explained in 3.1, while using for each subject a set of learning rates computed using leave-one (subject) out cross-validation. For *CMAC* and *CSEM*, the reported results are averages over 100 realizations of the experiment to account for fluctuations due to different realizations of the *RS*. For *CMAC*, the standard deviation of the results is shown as error bars. In the case of *CSEM*, the standard deviation of the solutions was very similar to that of *CMAC* and we decided to ignore them for visualization reasons.

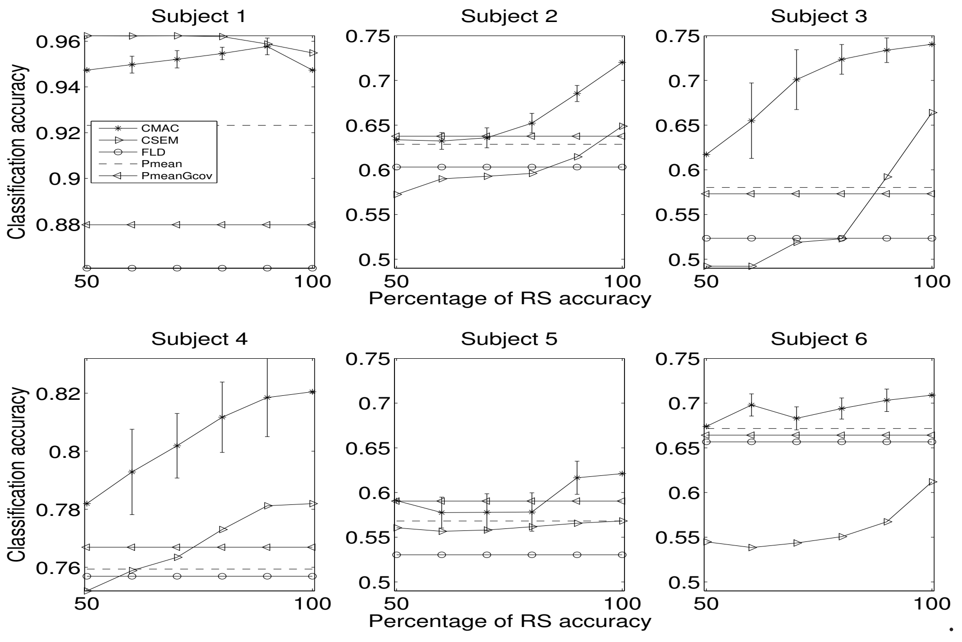

Figure 6: Classification accuracy (y-axis) as a function of the accuracy of the *RS* (x-axis) for all subjects. For *CMAC* the standard deviation of the solutions obtained is presented as an error bar.

We observe that in general all adaptive classifiers are able to outperform the static *LDA*. Considering the supervised scenarios, note that *CMAC* (100%) outperforms *CSEM* (100%). Only for subject number 1 *CSEM* (100%) is the best algorithm. Ignoring the supervised methods, we see also that *CMAC* is less sensible to non-optimal *RS* than *CSEM*. For subjects 3, 4 and 6 *CMAC* is the best algorithm for all considered *RS*, while for subjects number 2 and 5, it requires an accurate *RS* in order to improve wrt the unsupervised classifiers.

In Figure 7 we consider the cumulative classification accuracy against the trial number for *PmeanGcov*, *Pmean* and *CMAC* with optimal *RS*. *CMAC* is able to outperform the other methods not only at the end of the experiment (trial 140) but in general also at the end of the first test session (trial number 70). While for subject number 6 all methods show a similar trend, note that for subjects number 1 to 4, the difference in performance between *CMAC* and the other methods is bigger at trial 140 than at trial 70, showing that *CMAC* was able to adapt better after the pause between sessions. It is interesting to see that *CMAC* finishes the experiment with a general increasing trend, suggesting that the model continues a proper adaptation. Note in particular that for subject number 5 the performance of *CMAC* was worse at trial number 70 than the one of the other methods, but due to the ability to keep adapting after the pause, *CMAC* is the best algorithm at the end of the experiment.

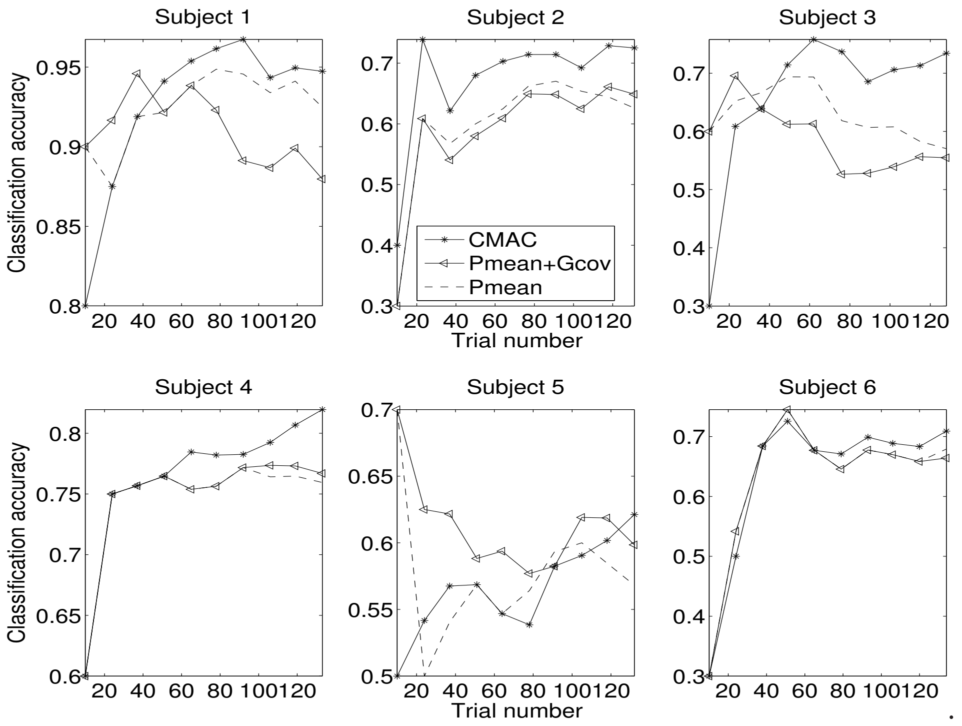

Figure 7: Cumulative classification accuracy against trial number for the *PmeanGcov*, *Pmean* and *CMAC*.

An interesting observation is that for some subjects, for example subject number 6, all methods perform similarly, while for other subjects, for example number 3, the increase in performance obtained using *CMAC* is significant. To understand this behavior, in figure 8 we show the distributions of the projected train data (discontinuous curves) and test data (continuous curves) onto the first and second CSP filters for subjects 6 and 3. Black and grey curves represent the two different classes. The boundary learned using the train data as well as the optimal boundary for the test data are also shown.

For subject number 6 we observe that the change in the distributions is very small, allowing every method to adapt to the changes. In constrast, the features of subject number 3 change notably between train and test. In particular, there is a clear rotation of the optimal boundary, which prevents *Pmean* to adapt properly. In this subject, although *PmeanGcov* should theoretically be able to correct for the rotation since it updates the global covariance matrix, we observe that it is not the case. The reason why *PmeanGcov* performs worse than CMAC could then be explained by the fact that, in addition to the rotation, the classes are swapped in the second filter (y-axis). Class information is therefore required to adapt to this type of changes, making it impossible for unsupervised methods such as *PmeanGcov*.

5 Related work and relations between methods.

In this section we provide a short description of the existing adaptive classification methods commonly used for BCI purposes, and we show the relationships between them. We also give a brief description of the binary Linear Discriminant Analysis (*LDA*) classifier.

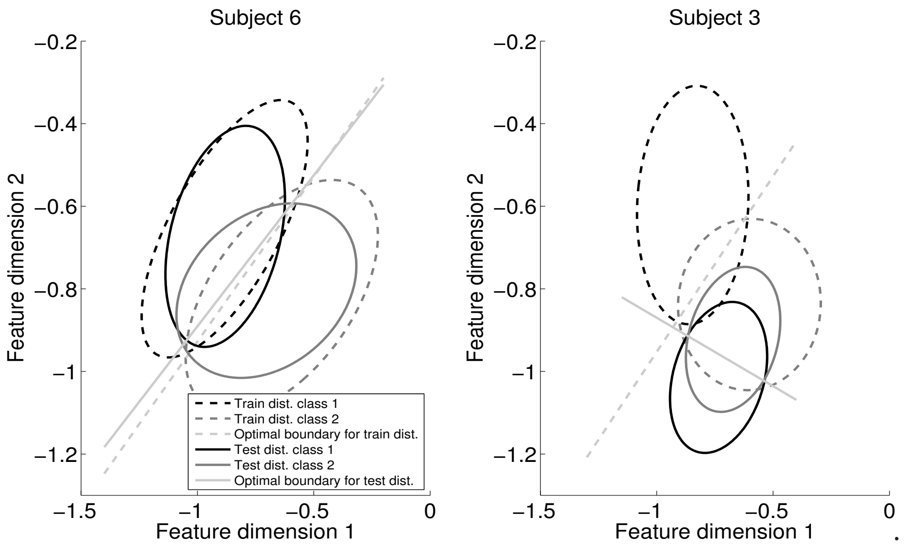

Figure 8: Projection of the data onto the first two CSP filters for subjects 6 and 3. Black and grey ellipses represent two different classes and discontinuous and continuous curves represent the train data and the test data respectively. Discontinuous and continuous straight lines show the optimal boundary for the train distributions and the test distributions respectively. For subject 6 (left) feature distributions do not change significantly. In contrast, for subject 3 (right) the optimal boundary rotates and the class labels are swapped in the vertical axis.

1. Binary Linear Discriminant Analysis (*LDA*).

   The binary *LDA* (Fukunaga, K. , 1990) is a classifier which is identified by a discriminant function $\mathcal{D}(\mathbf{x}) \in \mathbb{R}$ of the input feature vector $\mathbf{x} \in \mathbb{R}^n$. Denoting by $\boldsymbol{\mu}_k$ and Σ_k the means and covariance matrices of the train features of class $k \in \{1, 2\}$ respectively, and by $\Sigma = \frac{\Sigma_1 + \Sigma_2}{2}$ the mean of the covariance matrices, the discriminant function is defined by the equations

$$\mathcal{D}(\mathbf{x}) = [b, \mathbf{w}^\intercal] \begin{bmatrix} 1 \\ \mathbf{x} \end{bmatrix}, \tag{19}$$

$$\mathbf{w} = \Sigma^{-1} (\boldsymbol{\mu}_2 - \boldsymbol{\mu}_1), \tag{20}$$

$$b = -\mathbf{w}^\intercal \boldsymbol{\mu}, \tag{21}$$

$$\boldsymbol{\mu} = \frac{1}{2} (\boldsymbol{\mu}_1 + \boldsymbol{\mu}_2). \tag{22}$$

   Using this notation, $\mathbf{x}$ is classified as class 2 if $\mathcal{D}(\mathbf{x}) > 0$, and as class 1 otherwise. Note that $\mathbf{w} \in \mathbb{R}^n$ describes the vector of weights and $b \in \mathbb{R}$ describes the bias term of the discriminant function. Consequently, $\mathbf{w}$ determines the direction of the separating hyperplane while b the shift of the hyperplane wrt the origin.

2. Linear Discriminant Analysis with pooled mean adaptation (*Pmean*).

   Pmean (Vidaurre et al, 2010) is a discriminant-based unsupervised adaptive LDA algorithm which under the assumption of balanced classes, identifies (22) with the global mean of the data. In this way, (22) can be updated without any label information using the learning rule

$$\boldsymbol{\mu}' = (1 - \beta)\boldsymbol{\mu} + \beta\mathbf{x} \tag{23}$$

where $\boldsymbol{\mu}'$ is the updated $\boldsymbol{\mu}$, $\mathbf{x}$ is the new observed feature vector and $\beta \in [0, 1]$ is the learning rate controlling the adaptation. In this way the bias from the discriminant function gets updated through (21).

This kind of adaptation tracks changes in the bias of the discriminant function, consequently *Pmean* is able to adapt to shifts in feature space. Since the weights are not modified, this model can not account with changes in the direction of the separating hyperplane, as for example, rotations on feature space.

Note that *Pmean* can be considered a particular case of *CMAC* where $\beta_{-} = 0$ and $\beta_{\Sigma} = 0$.

3. Pmean with global covariance adaptation (*PmeanGcov*).

   PmeanGcov (Vidaurre et al, 2010) is a discriminant-based unsupervised adaptive LDA algorithm which in addition to the *Pmean* adaptation performs a sequential adaptation of the inverse of the global covariance. Under the assumption of balanced classes, we have that

$$\mathbf{w} = \Sigma^{-1}\left(\boldsymbol{\mu}_2 - \boldsymbol{\mu}_1\right) \propto \tilde{\Sigma}^{-1}\left(\boldsymbol{\mu}_2 - \boldsymbol{\mu}_1\right) := \tilde{\mathbf{w}},$$

   where $\tilde{\Sigma}$ is the global covariance matrix. Then, defining

$$\tilde{b} = -\tilde{\mathbf{w}}^{\mathsf{T}}\boldsymbol{\mu},$$

   we have that $\mathcal{D}(\mathbf{x}) \propto \tilde{\mathcal{D}}(\mathbf{x}) := \left[\tilde{b}, \tilde{\mathbf{w}}^{\mathsf{T}}\right]\begin{bmatrix} 1 \\ \mathbf{x} \end{bmatrix}$. This means that if the classes are balanced we obtain the same separating hyperplane using $\tilde{\Sigma}$ than using Σ. Using

$\tilde{\Sigma}$ has the advantage that it can be updated online without using class information. Furthermore, making use of the Woodbury matrix identity (matrix inversion lemma) we can directly update its inverse as

$$I = \tilde{\Sigma} - \frac{\mathbf{v}\mathbf{v}^{\mathsf{T}}}{\frac{1-\beta_{\Sigma}}{\beta_{\Sigma}} + \mathbf{x}^{\mathsf{T}}\mathbf{v}}, \tag{24}$$

$$\tilde{\Sigma'}^{-1} = \frac{I}{1-\beta_{\Sigma}}, \tag{25}$$

where $\tilde{\Sigma}$ is the global covariance, $\tilde{\Sigma'}^{-1}$ the updated inverse global covariance matrix, $\mathbf{v} = \tilde{\Sigma}^{-1}\mathbf{x}$, and $\beta_{\Sigma} \in [0, 1]$ is a learning rate controlling the adaptation of the covariance. This direct update of the inverse is recommended for online applications due to its efficiency.

The update of the inverse of the covariance allows for an update of (20), so *PmeanGcov* allows for the update of the weights and also the bias of the classifier. Consequently, this model has the potential power to adapt for shifts as well as for changes in the direction of the separating hyperplane.

Note that the update of the covariance in *PmeanGcov* is different from the class dependent covariance updates in *CMAC*. However, as previously explained, if the classes are balanced, using the pooled covariance in place of the mean of the class-wise covariance matrices results in the same separating hyperplane, so in that case *PmeanGcov* is equivalent with *CMAC* with $\beta_{-} = 0$.

4. Adaptive Linear Discriminant Analysis (*ALDA*).

ALDA (Blumberg et al, 2007) is a latent-variable-based unsupervised adaptive LDA algorithm in the sens that considers the user intention as a hidden variable, models the feature space as a GMM, and constructs a LDA classifier with the parameters estimated using EM. The batch optimization is performed using a sliding window of the last $\mathcal{M} \in \mathbb{N}$ trials. In this way, only the most recent trials take part in the optimization, allowing to model non stationary environments.

Since *ALDA* updates means and covariances, it performs an adaptation of all parameters included in the discriminant function, allowing like this to adapt for shifts as well as for rotation on feature space.

Note that since *CSEM* in the unsupervised scenario ($E^t = \frac{1}{2}\ \forall t$) is a sequential EM algorithm for GMM, we can identify *ALDEC* as the batch version of *CSEM*, and we can consider them as equivalent.

5. Adaptive Linear Discriminant Analysis with Error Correction (*ALDEC*).

   Similarly to our algorithm *CSEM*, in (Blumberg et al, 2007) the authors introduce a probabilistic model of a binary error signal, which corresponds to our RS term $p(I_k|Z, E)$. ALDEC performs implicit modeling of the decoding power DP (accuracy of the task classifier) and the reliability R of the RS. In contrast, in CSEM we explicitly include this information in the model and provide update rules for the means and covariances (6, 7) where the RS is included through the novel responsibilities (4). This allows us to recover both supervised and unsupervised cases. Further, this allows to include more realistic, single trial realizations of the RS. Notice that in (Blumberg et al, 2007) the RS is modeled as two delta peaks at R and $1 - R$ (see section 3.1).

6. Sequential EM (*SEM*).

SEM (Hasan et al, 2009) is a sequential version of EM for GMM. In this algorithm, the means and covariance matrices of the task related feature distributions are sequentially updated using

$$\boldsymbol{\mu}_I' = (1 - \beta_\mu \gamma_I)\boldsymbol{\mu}_I + \beta_\mu \gamma_I \mathbf{x}, \tag{26}$$

$$\boldsymbol{\Sigma}_I' = (1 - \beta_\Sigma \gamma_I)\boldsymbol{\Sigma}_I + \beta_\Sigma \gamma_I (\mathbf{x} - \boldsymbol{\mu}_I)(\mathbf{x} - \boldsymbol{\mu}_I)', \tag{27}$$

where $\boldsymbol{\mu}_I'$ and $\boldsymbol{\Sigma}_I'$ represent the updated means and covariance matrices respectively, $\mathbf{x}$ is the observed task related feature vector, γ_I the responsibilities computed using (8), and β_μ and β_Σ are *learning rates* which values decrease on size with the iteration number in order to reach convergence to the optimal static set of parameters. If our goal is to dynamically model a non stationary environment, we can relax the dependence of the learning rates value on the trial number, so $\beta_\mu \in [0, 1]$ and $\beta_\Sigma \in [0, 1]$.

Note that *SEM* is analytically equal to *CSEM* in the unsupervised scenario ($E^t = \frac{1}{2}\ \forall t$). Consequently, *SEM* is equivalent to the unsupervised *CSEM* and consequently to *ALDA*.

7. *CMAC* and *CSEM*.

CMAC and *CSEM* can not be reduced to the same class. If we compare the CMAC equations for the mean updates (15) and (16) with the CSEM equations (9), we see that CMAC contains additional terms involving the mean of the opposite class that are not in the CSEM update rule. These terms appear because CMAC constraints the sum and the differences of the class means.

6 Discussion

Our contribution in this article is two-fold. On the one hand, we introduced the probabilistic methodology to include a *Reinforcement Signal (RS)* in the adaptive BCI cycle, and we show that under the assumption of an informative *RS*, this model allows for a better estimation of the class probabilities (responsibilities) than the one obtained using only the task related features. On the other hand, we develop a novel update scheme for adaptive classification in BCI (*CMAC*), which can make use of the responsibilities computed using the proposed model, and is able to outperform state of the art adaptive classifiers.

It is interesting to note that in the supervised scenario, *CMAC* is able to improve a standard supervised adaptation (*supervised CSEM*), and also that even in the unsupervised scenario, *CMAC* has the potential to outperform other methods. However, the ability to get a big improvement wrt to other methods, clearly depends on the quality of the *RS*. As previously mentioned, such a *RS* can range from button presses delivered by the user (supervised), to measured muscular activity in an hybrid BCI (Leeb et al, 2010) or an ErrP classifier if we consider a pure BCI setting. Clearly, using muscular activity to detect erroneous performance can provide an accurate *RS*. It is important to note that in previous work (Llera et al, 2011) we have reported the possibility of relatively high ErrP classification rates (80 % of mean accuracy across 8 subjects), which agrees with the results presented previously by other researchers (Blankertz et al, 2004; Ferrez et al, 2008). Furthermore, in (Ferrez et al, 2008), it was also shown the high stability in ErrP detection across sessions. This facts make of this kind of *RS* a optimal candidate to include in online BCI experiments.

The improvement reported using the *CMAC* algorithm is due not only to the accuracy of the *RS*, but also to the introduction of an extra parameter β_- controlling the change in the difference between the means of the feature distributions. The optimal value for this parameter is clearly dependent on the accuracy of the estimated responsibilities. However, the simulations performed showed that the choice of this parameter value is not critical. In fact, we observed that setting $\beta_\Sigma = 0$, $\beta_+ = \beta_\mu \in [00.1]$, $\beta_- \in [0, 0.005]$, *CMAC* showed no significant difference wrt *Pmean* independently of the accuracy of the estimated responsibilities. For values $\beta_- \in [0.005, 0.03]$, the improvement wrt *Pmean* was proportional to the accuracy of the estimated responsibilities, and values $\beta_- > 0.03$ produced a decrease on performance wrt *Pmean*. The improvement wrt *Pmean* was obtained independently of β_+, which confirms the robustness of the method.

It is clear that the optimal choice of the learning rates is important to obtain good results for all subjects and all methods. There exist methods that can automatically adapt the learning rate to an optimal value that make a trade-off between accuracy for stationary data (low learning rate) and adaptivity to change (large learning rates) (Heskes et al, 1991b, 1992). We believe that such methods should be integrated in the adaptive BCI methodology.

An open question of considerable importance is how to generalize the proposed adaptive BCI methodology to non-binary tasks. Such learning tasks are more complex, since the error signal will indicate that an error has occurred, but will not provide information on what the correct output should have been. This type of learning paradigm is called reinforcement learning (Rescorla, 1967; Sutton et al, 1998; Dayan et al, 2001). An important future research direction is to integrate these reinforcement learning methods in on-line adaptive BCI.

Finally, we would like to remark that due to its generality, the proposed methodology has a broader application not restricted to BCI, for instance, in the construction of adaptive Spam filters (Zhou et al, 2005). In this environment the *RS* could be represented by the user getting a file out of or in the Spam folder.

Acknowledgments

The authors gratefully acknowledge the support of the Brain-Gain Smart Mix Programme of the Netherlands Ministry of Economic Affairs and the Netherlands Ministry of Education, Culture and Science.

References

Bishop, C. M.(2007). Pattern Recognition and Machine Learning. *Springer*.

Blankertz, B., Dornhege, G., Schäfer, C., Krepki, R., Kohlmorgen, J., Müller, K. R., Kunzmann, V., Losch, F & Curio, G. (2004). Boosting Bit Rates and Error Detection for the Classification of Fast-paced Motor Commands Based on Single-trial EEG Analysis. *IEEE Transactions on Biomedical Engineering*, vol. 51, no.6, 993 - 1002 .

Blankertz, B., Kawanabe, M., Tomioka, R., Hohlefeld, F., Nikulin, V. & Müller, K. R. (2008) Invariant Common Spatial Patterns: Alleviating Nonstationarities in Brain-Computer Interfacing. *Advances in Neural Information Processing Systems 20*, *MIT Press*,113–120.

Blumberg, J., Rickert, J., Waldert, S., Schulze-Bonhage, A., Aertsen, A., Mehring, C. (2007) Adaptive classification for brain computer interfaces. *29th Annual International Conference of the IEEE, Engineering in Medicine and Biology Society EMBS 2007*, pp. 2536–2539.

Chavarriaga, R., Ferrez, P.W. & Millán, J. del R. (2007). To Err Is Human: Learning from Error Potentials in Brain-Computer Interfaces *International Conference on Cognitive Neurodynamics, Shanghai, China*, 777–782.

Chavarriaga, R. & Millán, J. del R. (2010). Learning from EEG Error-related Potentials in Noninvasive Brain-Computer Interfaces. *IEEE Transactions on Neural Systems and Rehabilitation Engineering*, vol. 18, 381–388.

Dayan, P. & Abbott, L. F.(2001). Theoretical Neuroscience: Computational and Mathematical Modeling of Neural Systems *MIT Press*.

Ferrez, P.W. & Millán, J. del R. (2005). You Are Wrong!—Automatic Detection of Interaction Errors from Brain Waves. *Proceedings of the 19th International Joint Conference on Artificial Intelligence*, 1413 - 1418 .

Ferrez, P.W. (2007) Error-related EEG potentials in brain-computer interfaces. *Thèse Ecole polytechnique fédérale de Lausanne EPFL, no 3928*.

Ferrez, P. W. & Millán, J. del R. (2008). Error-Related EEG Potentials Generated during Simulated Brain-Computer Interaction. *IEEE Transactions on Biomedical Engineerings*, vol. 55, 3, 923 – 929.

Fukunaga, K. (1990) Introduction to Statistical Pattern Recognition. *Academic Press*.

Gan, J. G. (2006). Self-adapting BCI based on unsupervised learning. *3rd International Workshop on Brain-Computer Interfaces,Graz, Austria,Verslag*, 50–51.

Hasan, B. A. S. & Gan, J. Q. (2009). Unsupervised adaptive GMM for BCI. *International IEEE EMBS Conf. on Neural Engineering, Antalya, Turkey*, 295–298 .

Hasan, B.A.S. & Gan, J.Q. (2009b). Sequential EM for unsupervised adaptive Gaussian mixture model based classifier. *Machine Learning and Data Mining in Pattern Recognition, Lecture Notes in Computer Science, Springer Berlin / Heidelberg*, vol. 5632, 96–106.

Heskes, T., Gielen, S. & Kappen, H.J. (1991). Neural networks learning in a changing environment. *Artificial Neural Networks*, North-Holland, vol.1, 15–20.

Heskes, T. & Kappen, H.J. (1991b). Learning processes in neural networks *Physical Review A*, vol.44, 4, 2718–2726.

Heskes, T. & Kappen, H.J. (1992). Learning-parameter adjustment in neural networks. *Physical Review A*, vol.45, 8885–8893.

Kawanabe, M., Krauledat, M. & Blankertz, B. (2006). A bayesian approach for adaptive BCI classification *In Proceedings of the 3rd International Brain-Computer Interface Workshop and Training Course 2006*, *Verslag*, 54–55.

Krauledat M. (2008). Ph.d thesis. *Technische Universität Berlin, Fakultät IV – Elektrotechnik und Informatik.*

Lemm, S., Blankertz, B., Curio, G. & Müller, K. R. (2005). Spatio-Spectral Filters for Improved Classification of Single Trial EEG *IEEE Trans. Biomed. Eng*, vol. 52, 1541–1548.

Leeb, R. and Sagha, H. and Chavarriaga, R. and del R Millan, J. (2010). Multimodal Fusion of Muscle and Brain Signals for a Hybrid-BCI. *Engineering in Medicine and Biology Society (EMBC), 2010 Annual International Conference of the IEEE*, 4343 -4346.

Li, Y., & Guan, C. (2006) An Extended EM Algorithm for Joint Feature Extraction and Classification in Brain-Computer Interfaces. *Neural Computation*, vol.18, 11, 2730–2761.

Liu, G., Huang, G., Meng, J., Zhang, D. & Zhu, X. (2010) Improved GMM with parameter initialization for unsupervised adaptation of Brain-Computer interface. *International Journal for Numerical Methods in Biomedical Engineering*, vol.26, 6, 681–691.

Llera, A., van Gerven, M.A.J., Gómez, V., Jensen, O. & Kappen, H. J. (2011). On the use of interaction error potentials for adaptive brain computer interfaces. *Neural Networks*, vol. 24, 10, 1120 - 1127.

Millán, J. del R. (2004). On the Need for On-Line Learning in Brain-Computer Interfaces. *IEEE Proc. of the Int. Joint Conf. on Neural Networks*, vol.4, 2877 - 2882.

Müller-Gerking, J., Pfurtscheller, G. & Flyvbjerg, H.(1998) Designing optimal spatial filters for single-trial EEG classification in a movement task *Clinical Neurophysiology*, vol.110, 787–798.

Ramoser, H., Müller-Gerking, J. & Pfurtscheller, G. (1998). Optimal spatial filtering of single trial EEG during imagined hand movement. *IEEE Transactions on Rehabilitation and Engineering*, *8*, 441–446.

Reuderink, B., Farquhar, J., Poel, M. & Nijholt, A. (2011). A Subject-Independent Brain-Computer Interface based on Smoothed, Second-Order Baselining. *Proceedings of the 33st Annual International Conference of the IEEE Engineering in Medicine and Biology Society, EMBC 2011*, 4600–4604.

Samek, W., Vidaurre, C., Müller, K. R. & Kawanabe, M. (2012). Stationary Common Spatial Patterns for Brain-Computer Interfacing. *Journal of Neural Engineering*, *9* (*2*), 0260134.

Schmidt, N., Blankertz, B., Treder, M. S. (2012). Online detection of error-related potentials boosts the performance of mental typewriters. *BMC neuroscience*, *13*:19.

Shenoy, P., Krauledat, M., Blankertz, B., Rao, R. P. & Müller, K. R. (2006). Towards adaptive classification for BCI. *Journal of neural engineering*, *3*, R13-R23.

Sutton, R. S. & Barto, A. G.(1967). Pavlovian conditioning and its proper control procedures. *Psychological Review*, 74(1), 71–80.

Sutton, R. S. & Barto, A. G.(1998). Reinforcement Learning: An Introduction *MIT Press*.

Sykacek, P., Roberts, S. J. & Stokes M. (2004). Adaptive BCI Based on variational Kalman filtering: An empirical evaluation *IEEE Transactions on biomedical engineering*, vol.51, no.5, 719–727.

Tomioka, R., Hill, J.N., Blankertz, B. & Aihara, K. (2006) Adapting Spatial Filter Methods for Nonstationary BCIs *Proceedings of 2006 Workshop on Information-Based Induction Sciences (IBIS 2006)*, 65–70.

van Gerven, M. & Jensen, O. (2009). Attention modulations of posterior alpha as a control signal for two-dimensional brain-computer interfaces . *Journal of Neuroscience Methods*, *179*, 78 – 84.

Vidaurre, C., Schlöogl, A., Cabeza, R., Scherer, R., Pfurtscheller, G. (2006). A fully on-line adaptive BCI. *IEEE Transactions on Biomedical Engineering*, *6*, *53*, 1214–1219.

Vidaurre, C., Kawanabe, M., von Bünau, P., Blankertz, B. & Müller, K. R. (2010). Toward an unsupervised adaptation of LDA for Brain-Computer Interfaces. *IEEE Trans. Biomed. Eng*, vol.58, no.3, 587 – 597.

Vidaurre, C. & Blankertz, B. (2010b). Towards a Cure for BCI Illiteracy. *Brain Topogr.*, vol.23, 194–198.

Vidaurre, C., Sannelli, C., Müller, K. R. & Blankertz, B. (2010c). Machine-Learning Based Co-adaptive Calibration. *Neural Computation*,23(3), 791–816.

von Bünau, P., Meinecke, F. C., Scholler, S. & Müller, K. R. (2010). Finding Stationary Brain Sources in EEG Data. *Proceedings of the 32nd Annual Conference of the IEEE EMBS, 2010*, 2810 – 2813.

Wolpaw, J. R., Birbaumer, N., McFarland, D. J., Pfurtscheller, G. & Vaughan, T. M.

(2002). Brain-computer interfaces for communication and control. *Clinical neurophysiology*, *6-113*, 767–791.

Zhou, Yan and Mulekar, M.S. & Nerellapalli, P. (2005) Adaptive Spam Filtering Using Dynamic Feature Space. *17th IEEE International Conference on Tools with Artificial Intelligence (ICTAI'05)*, 302–309 .